DOI: 10.61782/fa.2025.0557

MECHANICALLY-OPEN AND ACOUSTICALLY-CLOSED MEMS LOUDSPEAKERS FOR IN-EAR APPLICATIONS

Chiara Gazzola[1*] **Filippo Perli**[1] **Fabrizio Cerini**[2] **Silvia Adorno**[2]
Pierrick Lotton[3] **Manuel Melon**[3] **Alberto Corigliano**[1]
[1] Department of Civil and Environmental Engineering, Politecnico di Milano, Italy
[2] STMicroelectronics, 20007 Cornaredo, Italy
[3] Laboratoire d'Acoustique de l'Université du Mans (LAUM), UMR 6613,
Institut d'Acoustique - Graduate School (IA-GS), CNRS, Le Mans Université, France

ABSTRACT

MEMS loudspeakers for in-ear applications have been attracting a growing interest in recent years, promising to overcome the limits in terms of form factor, power efficiency and cost of non-MEMS loudspeakers. The piezoelectric actuation principle is one of the most investigated, thanks to the introduction of high precision piezoelectric thin films with high electro-mechanical coupling coefficients in the microfabrication processes. This work presents a new set of high-performance piezoelectric MEMS speakers, consisting of PZT-driven thin plates properly shaped through a set of narrow slits. The latter serve the twofold purpose of enhancing the mechanical compliance of the speaker diaphragm and limiting the acoustic short-circuit between the speaker front and rear side. The diaphragm geometry, evolution of a design previously proposed by the Authors, is properly modified to improve the acoustic output and power efficiency. The proposed devices feature a Sound Pressure Level (SPL) at 30 V_{pp} greater than 108 dB SPL in the whole audible range, a Total Harmonic Distortion (THD) at 1 kHz at 94 dB SPL lower than 1% and a compact footprint of 4.5x4.5 mm^2. Experimental results are compared with a FEM-assisted lumped element model demonstrating a good match between them.

**Corresponding author*: *chiara.gazzola@polimi.it.*

Keywords: Piezoelectric thin films, MEMS, Microspeaker, Lumped Element Method, IEC 60318-4 coupler

1. INTRODUCTION

The integration of loudspeakers into devices such as smartphones, laptops, earphones, and hearing aids underscores their critical role in modern audio technology. The miniaturization of these systems into MEMS loudspeakers offers several advantages, including a compact form factor, low power consumption, and cost-efficient manufacturing, facilitating their widespread adoption in true wireless systems and in-ear applications, where power and space constraints are increasingly stringent.

To date, diaphragm actuation in MEMS loudspeakers can be achieved through electrodynamic (see *e.g.* [1, 2]), electrostatic (see *e.g.* [3, 4]), thermoacoustic (see *e.g.* [5, 6]), or piezoelectric (see *e.g.* [7–10]) forces. Among these, piezoelectric actuation has emerged as the most viable approach due to its ability to generate high driving forces at relatively low voltages. That is due to key technological advancements, including the development of piezoelectric materials with high electromechanical coupling, refined sputtering techniques enabling precise deposition in complex patterns, and the introduction of the mechanically-open and acoustically-closed (MOAC) design concept [8, 11]. This design strategy involves integrating a series of openings into the diaphragm to reduce its mechanical stiffness, thereby allowing for greater displacements. Simultaneously, these openings are designed so that the viscosity of the air within them limits the acoustic short-circuit between the front and rear side of the MEMS loudspeaker. Piezoelectric MEMS loudspeakers have achieved Sound Pressure Levels (SPL) exceeding 100 dB SPL in all the audible range, starting to close the performance gap with widely adopted non-MEMS loudspeakers. However, their sound pressure output per unit area has not yet reached its full potential.

This work presents a new set of high-performance piezoelectric MEMS speakers, whose diaphragms consists of PZT-driven thin plates separated by narrow slits. The devices were designed with the support of a FEM-assisted lumped element model [12], whose predictions are compared with in-ear acoustic measurements carried out on prototypes fabricated by STMicroelectronics (Cornaredo, Italy).

2. DESIGN CONCEPT

For a single-degree-of-freedom loudspeaker radiating in a cavity, the output pressure can be computed as [8]:

$$\Delta p = \gamma P_0 \frac{\Delta \mathcal{V}}{V_0} = \gamma P_0 \frac{d_{\max} S_{\text{eff}}}{V_0}, \tag{1}$$

where $\Delta\mathcal{V}$ is its volume displacement, given by the product of the speaker maximum displacement $d_{\max}$ and the speaker effective area S_{eff}, while γ is the adiabatic index (equal to 1.4 for dry air at 20 ° C), P_0 the ambient pressure and V_0 the volume of the cavity. The effective area of the speaker is computed as:

$$S_{eff} = \int_{\partial\Omega_f} \boldsymbol{\Phi} \cdot \boldsymbol{n} \, dS, \tag{2}$$

where $\boldsymbol{\Phi}$ is the modal shape function, $\partial\Omega_f$ is the surface area of the front side of the speaker and $\boldsymbol{n}$ its outward normal. Consequently, the parameters to address to maximize the speaker's acoustic performance are its maximum displacement and effective area, which are related respectively to the diaphragm mechanic stiffness and its movement type. The first can be reduced by implementing the MOAC design principle while the second can be maximized by encouraging the central part of the membrane to move like a piston. Following these design guidelines led to the diaphragms presented in Fig. 1, where a schematic cross-section of their structure is also given (Fig. 1c). The first design (Fig. 1a) consists of eight trapezoidal plates fabricated from a 13 µm-thick Epi-Poly silicon layer, partially coated with a 2 µm-thick Lead Zirconate Titanate (PZT) layer. These plates are connected to the central region of the MEMS loudspeaker through a network of elastic springs and are anchored to an external fixed frame. The eight plates are designed to be actuated synchronously, moving the diaphragm central part that they keep suspended like a piston. The mechanical gaps between adjacent trapezoidal plates extend from the fixed frame to the central region, effectively segmenting the PZT patches, which remain interconnected at the fixed frame. This distinct separation between plates, combined with the low stiffness of the elastic springs at their extremities, allows to mitigate the hardening effect that a clamped-clamped configuration would otherwise experience. The second device (Fig. 1b) features a reduced central region, leaving space for an additional set of elastic springs positioned along the extended trapezoidal plates. This modification aims to further enhance the maximum displacement of the diaphragm, albeit at the cost of deviating from an ideal piston-like motion. The two devices features a footprint of $4.5 \times 4.5\,\text{mm}^2$.

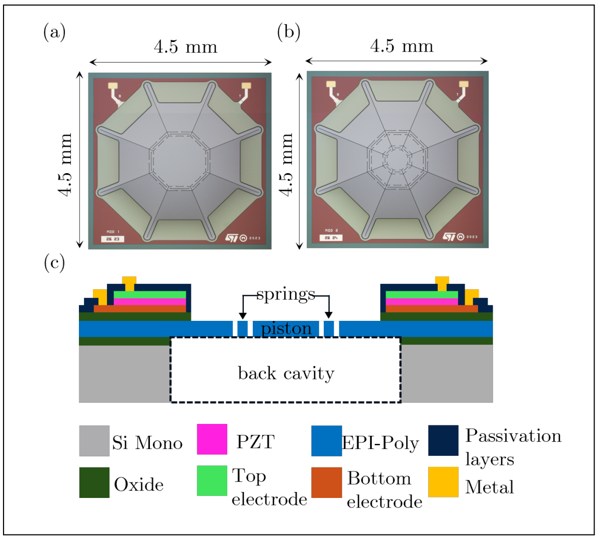

Figure 1. (a) Microscope optical images and (b) cross-sectional view of the proposed MEMS loudspeakers.

The proposed diaphragm geometries are an evolution of the design previously proposed by the Authors in [8]. Compared to the previous generation, the diaphragm structure is properly modified to improve the acoustic output with a halved piezoelectric capacitance, which is directly related to the power consumption. In particular, the air-gaps are reduced from 10 µm to 5 µm, to improve the sound pressure at low frequency by limiting the acous-

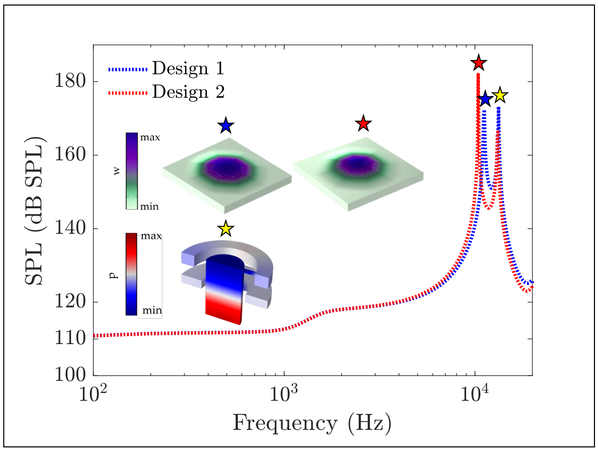

Figure 2. Equivalent circuit SPL predictions for design 1 and 2 at a bias voltage of 15 V_{DC} plus an alternating voltage of 30 V_{pp}. The insets report the loudspeakers deformed shape at their resonance frequency and the acoustic pressure distribution at the half wavelength resonance of the ear simulator.

tic short-circuit. The piezoelectric capacitance is reduced from 70 nF to 35 nF.

3. NUMERICAL RESULTS

The acoustical performances of the proposed loudspeakers are simulated through the FEM-assisted lumped element model reported in [12]. In particular, a FEM prestressed eigenfrequency analysis is exploited for the derivation of the electro-mechanical parameters whereas acoustical parameters are computed through analytical formulas.

The acoustic performance for a bias voltage of 15 V_{DC} plus an alternating voltage of 30 V_{pp} are reported in Fig. 2. The actuated loudspeaker mode, occuring at 11.6 kHz for design 1 and at 10.7 kHz for design 2, determines the first peak of the SPL curves. The second peak is instead due to the half wavelength resonance of the ear simulator. The simulations predict a SPL greater than 110 dB SPL from 100 Hz onwards and a relatively flat response at low frequency, due to the reduced slit width.

4. EXPERIMENTAL RESULTS

The numerical SPL predictions are compared with experimental measurements carried out on nine prototypes of

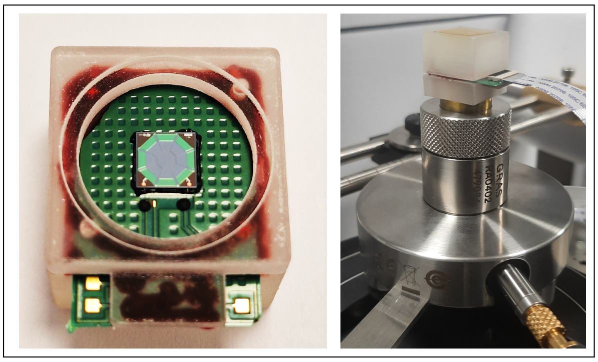

Figure 3. Fabricated microspeaker mounted on a custom PCB and coupled with the package for in-ear acoustic tests (left). Device Under Test (DUT) mounted on the ear simulator G.R.A.S. RA0402 (right).

the proposed microspeakers, fabricated by STMicroelectronics. For experimental tests, the device is mounted on a custom printed circuit board (PCB) and coupled with an acrylonitrile butadiene styrene (ABS) thermoplastic package composed of a back chamber of 1 cm^3 and a front adapter of 1 mm height to connect the speaker with the ear simulator (Fig. 3).

The experimental SPL curves for a bias voltage of 15 V_{DC} plus an alternating voltage of 30 V_{pp} is reported in Fig. 4, for design 1 and 2. The acquisition is stopped at 10 kHz to avoid the break-up of the prototypes. Overall, the numerical vs experimental matching is good (overestimation at 100 Hz of 2.3 dB SPL for design 1 and 2.7 dB SPL for design 2). As reference, the experimental SPL curve for the design of the previous generation [12] is reported in the same figure with black solid line. It can be confirmed that the reduction of the slit width from 10 µm to 5 µm leads to a significant SPL improvement at low frequency (+5 dB SPL at 100 Hz). Moreover, despite the halved piezoelectric surface area, the output pressure is overall higher for the new devices.

The THD has also been evaluated at 1 kHz at 94 dB SPL, obtaining 0.68% for design 1 and 0.72% for design 2 (previous design 1.5%).

5. CONCLUSIONS

Two full-range piezoelectric MEMS loudspeakers for in-ear applications are designed, simulated, fabricated and experimentally characterized. The good match between

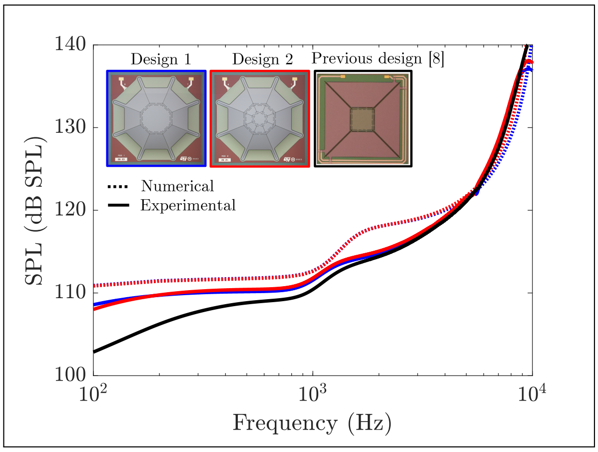

Figure 4. (a) Comparison between numerical (dotted lines) and experimental (solid lines) SPL frequency spectra for a bias voltage of 15 V_{DC} plus 30 V_{pp}, for design 1, design 2 and the design reported in [8].The acquisition is stopped at 10 kHz to avoid the break-up of the prototypes.

simulations and experiments demonstrates that, with respect to the previous generation, the proposed designs gain up to 5 dB SPL at low frequency and more than halve the previous THD, while keeping the same device footprint and a halved piezoelectric surface area.

6. REFERENCES

[1] I. Shahosseini, E. Lefeuvre, J. Moulin, E. Martincic, M. Woytasik, and G. Lemarquand, "Optimization and microfabrication of high performance silicon-based mems microspeaker," *IEEE Sensors Journal*, vol. 13, no. 1, pp. 273–284, 2013.

[2] I. Shahosseini, E. L. M. Woytasik, J. Moulin, X. Leroux, S. Edmond, E. Dufour-Gergam, A. Bosseboeuf, G. Lemarquand, and V. Lemarquand, "Towards high fidelity high efficiency mems microspeakers," *IEEE SENSORS*, 2010.

[3] M. V. Garud and R. Pratap, "A novel mems speaker with peripheral electrostatic actuation," *Journal of Microelectromechanical Systems*, vol. 29, no. 4, pp. 592–599, 2020.

[4] C. Sano, M. Ataka, G. Hashiguchi, and H. Toshiyoshi, "An electret-augmented low-voltage mems electrostatic out-of-plane actuator for acoustic transducer applications," *Micromachines*, vol. 11, no. 3, p. 267, 2020.

[5] H. Tian, T. Ren, D. Xie, Y. Wang, C. Zhou, T. Feng, D. Fu, Y. Yang, P. Peng, L. Wang, and L. Liu, "Graphene-on-paper sound source devices," *IEEE 34th International Conference on Micro Electro Mechanical Systems (MEMS)*, vol. 6, no. 5, pp. 4878–4885, 2011.

[6] W. Fei, J. Zhou, and W. Guo, "Low-voltage driven graphene foam thermoacoustic speaker," *Small*, no. 19, p. 2252–2256, 2014.

[7] H.-H. Cheng, S.-C. Lo, Z.-R. Huang, Y.-J. Wang, M. Wu, and W. Fang, "On the design of piezoelectric mems microspeaker for the sound pressure level enhancement," *Sensors and Actuators A: Physical*, vol. 306, p. 111960, 2020.

[8] C. Gazzola, V. Zega., F. Cerini, S. Adorno, and A. Corigliano, "On the design and modeling of a full-range piezoelectric mems loudspeaker for in-ear applications," *Journal of Microelectromechanical Systems*, vol. 99, pp. 1–12, 2023.

[9] R. Liechti, S. Durand, T. Hilt, F. Casset, C. Dieppedale, and M. Colin, "High performance piezoelectric mems loudspeaker based on an innovative wafer bonding process," *Sensors and Actuators A: Physical*, vol. 358, p. 114413, 2023.

[10] F. Stoppel, J. Fankhänel, T. Giese, C. Eisermann, I. Pieper, and F. Lofink, "Highly miniaturized 115 db full-range mems loudspeaker for in-ear applications," *Sensors and Actuators A: Physical*, p. 116373, 2025.

[11] F. Stoppel, A. Männchen, F. Niekiel, D. Beer, T. Giese, and B. Wagner, "New integrated full-range mems speaker for in-ear applications," *IEEE Micro Electro Mechanical Systems (MEMS)*, 2018.

[12] C. Gazzola, V. Zega, A. Corigliano, P. Lotton, and M. Melon, "A reduced-order-model-based equivalent circuit for piezoelectric micro-electro-mechanical-system loudspeakers modeling," *The Journal of the Acoustical Society of America*, vol. 155, no. 2, pp. 1503–1514, 2024.